



## Synthesis of polyethyleneimine modified polyurethane foam for removal of Pb(II) ion from aqueous solution

Zhenjiang Zhang<sup>a,b</sup>, Lili Zhu<sup>a,b,\*</sup>, Zhongwei Zhang<sup>a</sup>, Linyan Sun<sup>a</sup>, Yan Shi<sup>a</sup>, Lijun Xie<sup>a</sup>, Dongyan Xu<sup>a</sup>, Juan Jin<sup>a,b</sup>, Zhongxin Xue<sup>a,b</sup>, Xiaolin Ma<sup>a</sup>

<sup>a</sup>College of Chemistry and Materials Science, Ludong University, Yantai 264025, China, Tel. +86 535 6696162, email: zhangzhj365@126.com (Z. Zhang), zhulili246@163.com (L. Zhu), 863767171@qq.com (Z. Zhang), 2519061355@qq.com (L. Sun), 1075963876@qq.com (Y. Shi), 1019934820@qq.com (L. Xie), 1098308169@qq.com (D. Xu), jinjuan8341@163.com (J. Jin), ldxuezx@126.com (Z. Xue), 3099676946@qq.com (X. Ma)

<sup>b</sup>Collaborative Innovation Center of Shandong Province for High Performance Fibers and Their Composites, Ludong University, Yantai 264025, China

Received 9 October 2018; Accepted 5 May 2019

### ABSTRACT

A novel adsorbent based on polyurethane foam (PUF) with high density of amino groups was studied for Pb(II) removal. Polyethyleneimine (PEI) was used as functional reagent to modify the surface of PUF. The PEI modified PUF (PEI-PUF) was characterized by FTIR, SEM, XPS and elementary analysis and used for removal of Pb(II) ion from aqueous solution. The effects of equilibrium time, pH of the solution, initial Pb(II) concentration and temperature were investigated. PEI-PUF-10 and PEI-PUF-30 with different PEI content exhibited superior adsorption performance of Pb(II). Compared with PEI-PUF-10, PEI-PUF-30 has a faster adsorption rate, shorter equilibrium time and higher adsorption capacity, which may be due to the high content of PEI and the easily accessible active sites. The maximum adsorption capacity of Pb(II) on PEI-PUF-10 and PEI-PUF-30 were 98.1 and 183.0 mg g<sup>-1</sup>, respectively. The adsorption of Pb(II) on PEI-PUF was highly pH dependent and endothermic. After five cycles of adsorption/desorption, the adsorption capacity of Pb(II) on PEI-PUF-30 only showed a slight loss, which indicated that the adsorbents can be regenerated and reused for practical application.

*Keywords:* Polyurethane foam; Polyethyleneimine; Heavy metal removal; Pb(II) adsorption

### 1. Introduction

Nowadays, heavy metal pollution of aquatic environments has attracted great attention due to their toxic effect on human beings and ecological systems [1]. Unlike some organic pollutants, toxic heavy metals are not biodegradable and tend to accumulate in an ecosystem through the food chain [2–4]. Among them, lead (Pb) is one of the most toxic heavy metal environmental pollutants [5]. Even very low concentration of Pb(II) is detrimental to human brain, blood circulation, kidneys and reproductive system and can cause serious diseases [6]. The maximum contaminant level

for lead in drinking water has been set at 15 µg L<sup>-1</sup> according to the United States Environmental Protection Agency (USEPA) [7]. Therefore, it is important to eliminate Pb(II) from wastewater before discharged into the environment.

Various techniques have been studied for removal of Pb(II) from water, such as chemical precipitation, membrane filtration, ion exchange, solvent extraction and adsorption [8,9]. Adsorption is recognized as an easy and effective method owing to its low cost, simplicity for design, easy operation and reversibility [10–12]. Nowadays, a variety of adsorbents have been developed for Pb(II) removal, such as activated carbon [13], clay minerals [14], carbon nanotubes [15], zeolite [16], polymer resin [17], silica gel [18] and polyurethane foam (PUF). This paper focuses on the study of low-cost PUF material to develop a novel

\*Corresponding author.

high adsorption efficiency material. PUF is an excellent sorbent material with cellular structure, remarkable chemical and thermal resistance, and ability to retain various types of substances due to the presence of polar and non-polar groups in their structures [19]. These features allow them to be easily separated from aqueous solutions, and make them have remarkable mass transfer properties and rapid adsorption rates [20].

Initially, pristine PUF without modified were widely used to separate a wide variety of inorganic and organic species from aqueous media [19]. However, the low adsorption efficiency of pristine PUF limited their practical applications [20]. Therefore, the modification of PUF is essential for improving its adsorption efficiency. Modified PUF has been used for removal of oil [21], dyes [22–24] and metal ions [25] from aqueous solutions. For the adsorption of heavy metal ions, different types of adsorbents based on PUF, such as loaded PUF, chemically modified PUF and composite PUF have been studied [25]. Burham [26] prepared 2-aminoacetylthiophenol modified polyurethane foam for selective separation and preconcentration of Pb(II) with adsorption capacity of 10.75 mg g<sup>-1</sup>. Sone et al. [27] prepared alginate/polyurethane composite foams by reaction of sodium alginate with prepolymer of polyurethane for selectively adsorbing Pb(II) from contaminated water. The adsorbent was hydrophilic, flexible, durable and easy to produce. The adsorption capacity of the adsorbent was 16.0 μmol g<sup>-1</sup>. Jang et al. [28] prepared hydroxyapatite/polyurethane composite foams and investigated their removal capability of Pb(II) from aqueous solutions. The maximum adsorption capacity was 150 mg g<sup>-1</sup> for the composite foam with 50 wt.% hydroxyapatite content. However, the adsorption capacities of modified PUF are less than satisfactory for removal of Pb(II) from wastewater. Moreover, the stability and reusability of modified PUF needs to be improved.

Polyethyleneimine (PEI) exhibits strong adsorption ability for heavy metals due to the presence of a large number of primary and secondary amine functional groups in the molecule [29]. However, the high solubility of PEI in water makes it difficult to achieve liquid/solid separation. Therefore, PEI molecules with amine groups are usually grafted or coated on solid support to act as an effective adsorbent. The PEI modified adsorbents can provide plenty of functional groups for heavy metals adsorption and enhance the adsorption capacity. If we fabricate the PEI modified PUF (PEI-PUF), it would be expected to be effective for removing Pb(II) from aqueous solution. Moreover, PUF is an excellent adsorbent support with flexibility, opened macrostructure, good mechanical properties and low commercial cost. In this paper, a novel PEI-PUF adsorbent was developed with PEI coated on the surface of PUF. The obtained PEI-PUF has both advantages of PUF and PEI, and can effectively remove Pb(II) from waste water.

## 2. Experimental section

### 2.1. Materials

The open-cell polyether-type PUF having density of 50 kg m<sup>-3</sup> was kindly supplied from Liming Research & Design Institute of Chemical Industry Co., Ltd. (China). Branched PEI (molecular weight of 10000) was purchased from Sig-

ma-Aldrich. The stock solution of Pb(II) was prepared from lead nitrate (Pb(NO<sub>3</sub>)<sub>2</sub>) of analytical grade reagent. The other chemicals were analytical grade reagents.

### 2.2. Preparation of PEI modified PUF (PEI-PUF)

Pristine PUF was etched with chromic acid solution (H<sub>2</sub>SO<sub>4</sub> 100 g L<sup>-1</sup>, CrO<sub>3</sub> 100 g L<sup>-1</sup>) for 1 min at room temperature as a pretreatment. And then the foam was rinsed sufficiently with distilled water and dried in an oven at 60°C. 1.0 g of etched PUF was immersed in 100 mL of DMF solution containing PEI (10 or 30 g L<sup>-1</sup>) and shaken for 24 h at 25°C. Then the mixture was immediately transferred into 100 mL of 2.5% (w/v) glutaraldehyde solution with shaking at 25°C for 2 h, followed by washing with plenty of distilled water. The foam was dried in a vacuum. The PEI-PUF with PEI concentration of 10 and 30 g L<sup>-1</sup> were denoted as PEI-PUF-10 and PEI-PUF-30, respectively.

### 2.3. Characterization

Fourier transform infrared (FT-IR) analysis was conducted with a Bruker VECT OR 22/N spectrometer (German). Elementary analysis was performed by VarioEL. The morphology of the samples was observed using ultra-high resolution field emission scanning electron microscopy (FESEM, SU8010, Hitachi, Japan). The zeta potential of the samples was measured by the Zetasizer (Nano-ZS90, Malvern) in water over a pH range from 1 to 12. The pH was adjusted with HNO<sub>3</sub> and NaOH, respectively. The X-ray photoelectron spectroscopy (XPS) was recorded by ESCALAB Xi+ (Thermo Fisher Scientific). The concentration of Pb(II) was determined by flame atomic absorption spectrophotometer (AA240, VARIAN).

### 2.4. Batch adsorption experiments

The adsorption behaviors of prepared adsorbents were studied by the batch method, in which 0.05 g of adsorbent was shaken with 20 mL of Pb(II) solution. After reaching equilibrium, the concentration of Pb(II) was determined by flame atomic adsorption spectrophotometer. The amount of adsorbed Pb(II) was calculated by a mass balance between the initial and equilibrium concentrations. The effects of shaking time, pH, initial Pb(II) concentration and temperature were studied.

Each experiment was studied at 25°C except temperature experiment. All batch experiments were carried out in duplicate under the same conditions, and the relative error between duplicates was less than 5%. The results were reported as mean values.

### 2.5. Methods

Pseudo-first-order and pseudo-second-order kinetics models were used to fit the experimental data obtained. The Lagergren pseudo-first-order equation [30] is expressed as Eq. (1).

$$\log(q_e - q_t) = \log q_e - \frac{k_1}{2.303} t \quad (1)$$

The pseudo-second-order model of Ho [31] is expressed as Eq. (2).

$$\frac{t}{q_t} = \frac{1}{k_2 q_e^2} + \frac{t}{q_e} \quad (2)$$

where  $q_t$  and  $q_e$  are the amounts of adsorbed Pb(II) at time  $t$  and equilibrium, respectively.  $k_1$  is the rate constant of pseudo-first-order adsorption.  $k_2$  is the rate constant of pseudo-second-order adsorption. The kinetics parameters of  $q_e$ ,  $k_1$  and  $k_2$  can be calculated by plotting of  $q_t$  versus  $t$ .

The Langmuir isotherm is frequently used single-component adsorption model. Langmuir model assumes that the adsorption occurs on a homogeneous surface by monolayer adsorption without interaction between adsorbed molecules. The Langmuir equation is expressed as Eq. (3)

$$\frac{C_e}{q_e} = \frac{C_e}{q_m} + \frac{1}{b q_m} \quad (3)$$

where  $C_e$  ( $\text{mg L}^{-1}$ ) is the equilibrium concentration of Pb(II);  $q_e$  ( $\text{mg g}^{-1}$ ) is the amount of Pb(II) adsorbed at equilibrium;  $q_m$  ( $\text{mg g}^{-1}$ ) is the maximum adsorption capacity of Pb(II); and  $b$  ( $\text{L mg}^{-1}$ ) is the Langmuir constant related to the energy of sorption.

Thermodynamic studies were investigated over a temperature range of 288–308 K and calculations were performed to obtain parameters such as Gibbs free energy change ( $\Delta G$ ), enthalpy change ( $\Delta H$ ) and entropy change ( $\Delta S$ ) for the adsorption process.

## 2.6. Regeneration experiments

To investigate the regeneration of adsorbents, 0.1 mol L<sup>-1</sup> EDTA was used as the regeneration solution. 0.05 g of PEI-PUF-30 was mixed with 20 mL of 100 mg L<sup>-1</sup> Pb(II) solution and shaken for 80 min. Then the Pb(II) loaded PEI-PUF-30 was immersed in 10 mL of 0.1 mol L<sup>-1</sup> EDTA solution for 80 min to be desorbed. After that, PEI-PUF-30 was separated from the regeneration solution and washed with water. Then PEI-PUF-30 was dried in vacuum for the next adsorption cycle. Five consecutive adsorption-desorption cycles were conducted to explore the reusability of PEI-PUF. After each cycle, the adsorption amount was determined.

## 3. Results and discussion

### 3.1. Characterization

The FTIR spectra of pristine PUF, PEI-PUF-10 and PEI-PUF-30 are shown in Fig. 1. FTIR spectrum of pristine PUF shows a broad band at 3670–3200 cm<sup>-1</sup>, which is attributed to N-H stretching vibration. The bands at 1709 cm<sup>-1</sup> and 1656 cm<sup>-1</sup> are corresponding to C=O stretching vibration of -NHCOO- group and -NHCONH- group, respectively [22]. FTIR spectra of PEI-PUF-10 and PEI-PUF-30 (Fig. 1b and Fig. 1c) show much broader band at 3670–3000 cm<sup>-1</sup> than that of pristine PUF, which may be due to the superposition of NH<sub>2</sub> and NH stretching vibration of PEI and NH stretching vibration of PUF skeleton. The band at 1090 cm<sup>-1</sup> is ascribed to the stretching vibration of C-O-C, and this band is used as internal standard peak. The integrated

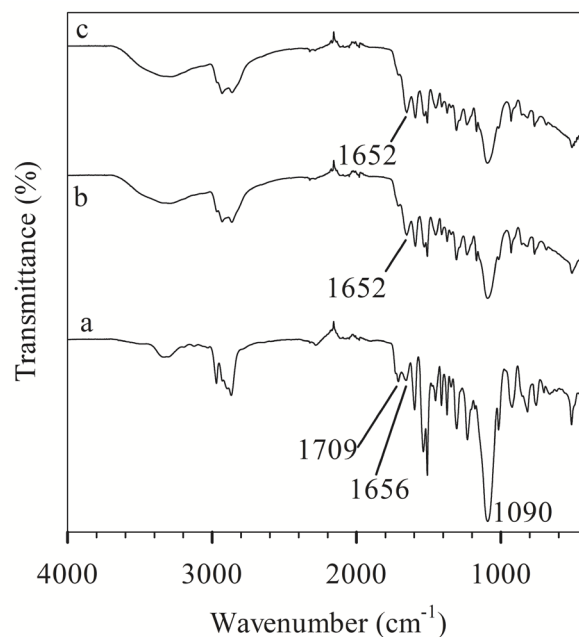


Fig. 1. FTIR spectra of pristine PUF (a), PEI-PUF-10 (b) and PEI-PUF-30 (c).

Table 1

Elementary analysis of pristine PUF, PEI-PUF-10 and PEI-PUF-30

Sample	N (wt. %)	C (wt. %)	H (wt. %)
Pristine PUF	3.99	63.38	8.51
PEI-PUF-10	8.47	59.35	8.34
PEI-PUF-30	10.23	59.07	8.45

intensity ratio of  $I_{1656}/I_{1090}$  was only 0.05 for pristine PUF.  $I_{1656}$  and  $I_{1090}$  are the peak area of the bands centered at 1656 and 1090 cm<sup>-1</sup>, respectively. However, the values of  $I_{1652}/I_{1090}$  for PEI-PUF-10 and PEI-PUF-30 were 0.24 and 0.32, respectively. The increased intensity of the band at 1652 cm<sup>-1</sup> may be due to the C=N stretching vibration which was produced by the reaction between glutaraldehyde and PEI [32,33]. Therefore, the combination band at 1652 cm<sup>-1</sup> for PEI-PUF-10 and PEI-PUF-30 was ascribed to C=O stretching vibration of -NHCONH- plus C=N stretching vibration.

The elemental composition of pristine PUF, PEI-PUF-10 and PEI-PUF-30 were analyzed, and the results are shown in Table 1. The nitrogen contents of PEI-PUF-10 and PEI-PUF-30 are much higher than that of pristine PUF, which is due to the functionalization of PEI. The characterization of FTIR spectra and elementary analysis indicated that PEI has been successfully introduced into the support skeleton. Moreover, the nitrogen content of PEI-PUF-30 is higher than that of PEI-PUF-10, which indicated that the PEI content of PEI-PUF-30 is higher than that of PEI-PUF-10.

The morphology of pristine PUF, etched PUF and PEI-PUF-30 was characterized by FESEM, as shown in Fig. 2. All the three kinds of foams possess opening cell structures. The surface of pristine PUF is smooth and flat. For etched PUF,



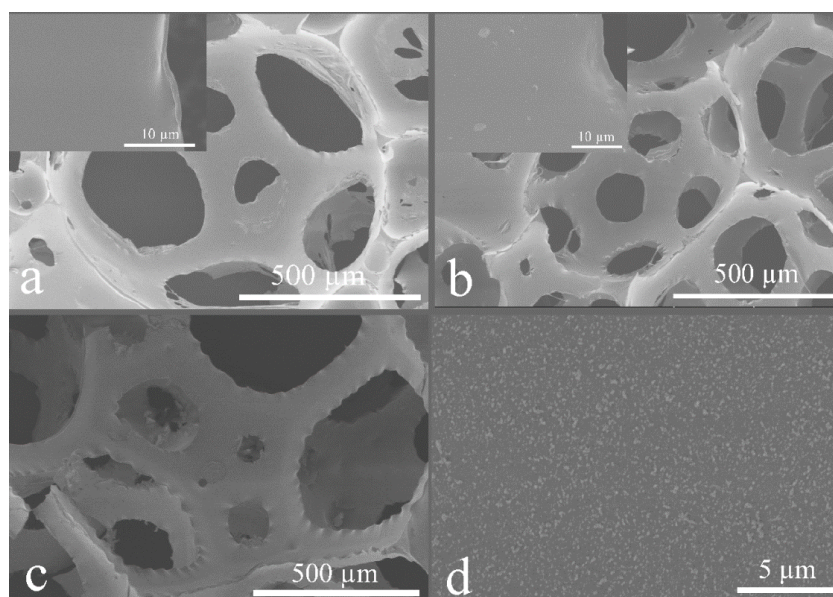


Fig. 2. FESEM images of pristine PUF (a), etched PUF (b) and PEI-PUF-30 (c, d).

the low-magnification SEM image shows similar structure with pristine PUF. However, the high-magnification SEM image shows some micrometer scale structures on the surface. The surface roughness of etched PUF increased compared with pristine PUF, which enhancing the interaction area [34]. For PEI-PUF-30, the edge of open cell is roughness (Fig. 2c), and there are many nanoscale structures on modified PUF surface (Fig. 2d), which may be due to the cross-linked PEI.

The XPS total survey spectra of pristine PUF, etched PUF and PEI-PUF-10 are illustrated in Fig. 3a. The presence of large amounts of the elements C, N and O in the three materials was evidenced by the photoelectron lines in the wide scan spectrum with binding energies at 285, 399 and 531 eV, attributed to C 1s, N 1s and O 1s, respectively. The C 1s spectrum of pristine PUF displayed three peaks (shown in Fig. 3b) at 284.8eV, 286.3eV and 289.2eV, which were attributed to C–C, C–O (or C–N) and –NHCOO–bonds respectively [35–37]. After etched with chromic acid solution, the C 1s spectrum of etched PUF was decomposed into three peaks (shown in Fig. 3c). The new peak at 288.7 eV was attributed to the O–C=O bond. It represented the existence of carboxyl groups which increased the interaction between etched PUF and PEI, such as hydrogen bond and electrostatic interaction. Similar result was found by Zhu [38], who reported that hydroxyl and carboxyl groups appeared on the surface of etched PUF. The C 1s spectrum of PEI-PUF-10 was decomposed into four peaks (shown in Fig. 3d). The new peak at 286.5 eV represented the C=N bond which produced by the reaction between glutaraldehyde and PEI. The XPS results were consistent with the results of FT-IR analysis.

### 3.2. Effect of pH on Pb(II) adsorption

The initial pH value of Pb(II) solution had a strong effect on the adsorption behavior of PEI-PUF-10 and PEI-PUF-30,

as shown in Fig. 4. The investigated initial pH range was from 1.1 to 5.7 in order to prevent the precipitation of Pb(II) at higher pH values. Most Pb(II) species exist as  $Pb^{2+}$  in this pH range, and only a small portion of  $Pb(OH)^+$  ions are present when pH approaching 6.0 [39]. When the pH of solution is above 8,  $Pb(OH)_2$  starts to appear [7]. It can be seen from Fig. 4, there are almost no adsorption of Pb(II) on PEI-PUF-10 and PEI-PUF-30 at pH 1–2. Then the adsorption amount increased sharply with the pH increase at pH 2–4 and slowly at pH 4–5.7. To better understand the influence of pH on the adsorption capacity, the zeta potentials of PEI-PUF-10 and PEI-PUF-30 were determined and shown in Fig. 5. The pH of zero charge point ( $pH_{zcp}$ ) was estimated. Both PEI-PUF-10 and PEI-PUF-30 have  $pH_{zcp}$  values around 2.5. It indicated that the surfaces of PEI-PUF-10 and PEI-PUF-30 are positively charged at pH values lower than 2.5. That was due to the protonation of surface functional groups of PEI-PUF-10 and PEI-PUF-30 which have a large number of primary and secondary amine groups. The competitive adsorption was occurred between the protons and Pb(II) for the same adsorption sites at high  $H^+$  concentration. Therefore, the adsorption of Pb(II) was significantly hindered at low pH condition due to less availability of active sites for adsorption of Pb(II). When pH higher than 2.5, the surfaces of PEI-PUF-10 and PEI-PUF-30 are negatively charged. The chelating ability of primary and secondary amine groups for Pb(II) was enhanced, which leading to the adsorption amount increase. In addition, electrostatic attraction also led to an increase in the adsorption amount. The adsorption mechanism was mainly complexation followed by electrostatic interaction. The maximum adsorption amount was obtained at pH 5.7. Therefore, the other all experiments were carried out at pH 5.7.

### 3.3. Adsorption kinetics

The solid points in Fig. 6 show the effect of shaking time on the adsorption of Pb(II) by PEI-PUF-10 and PEI-PUF-30.

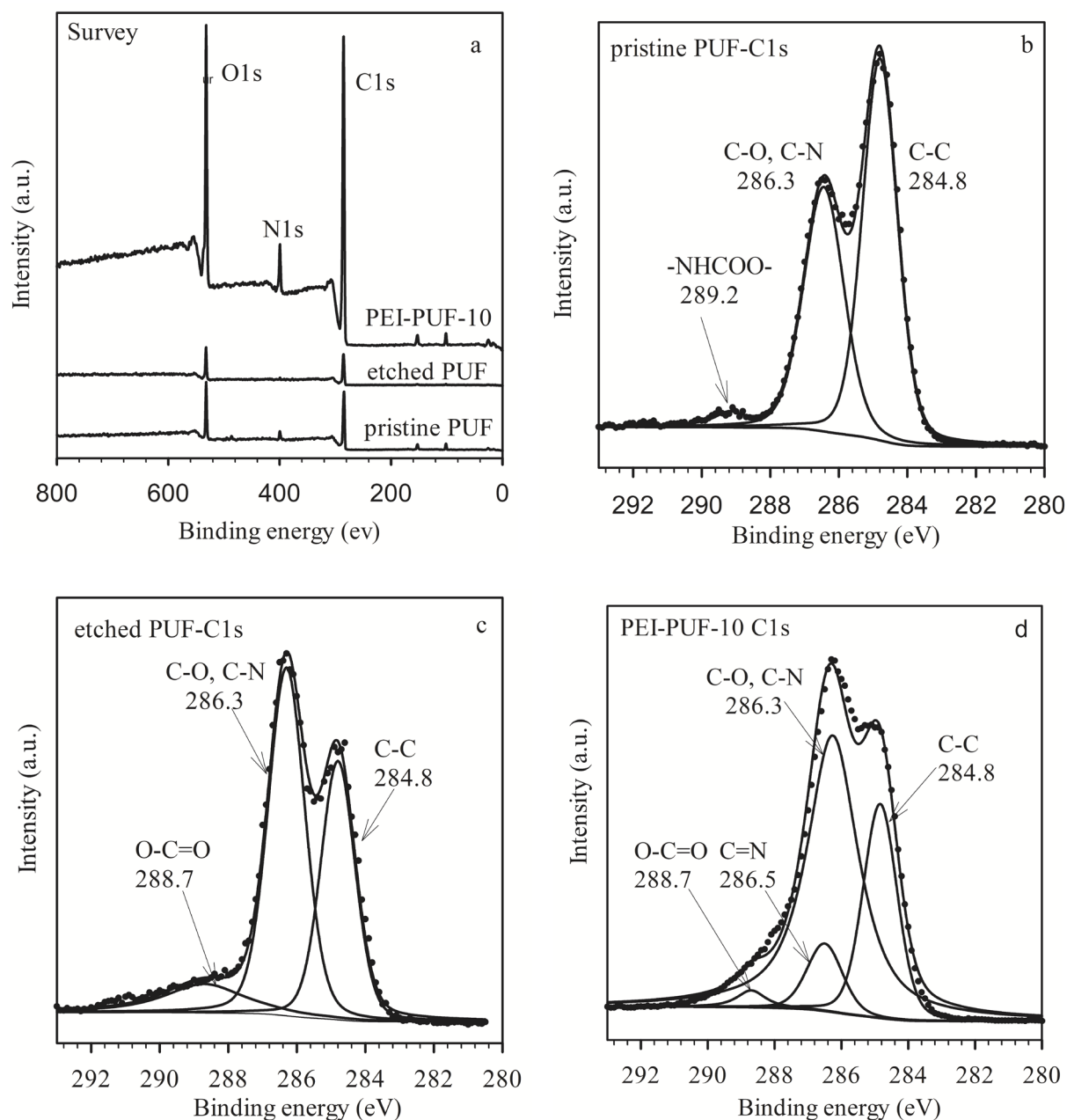


Fig. 3. The XPS total survey spectra of pristine PUF, etched PUF and PEI-PUF-10 (a), and the C 1s spectra of pristine PUF (b), etched PUF (c) and PEI-PUF-10 (d).

The adsorption of Pb(II) was fast at initial times and then approached equilibrium at longer times. The adsorption equilibriums were attained at 80 min for PEI-PUF-10 and 20 min for PEI-PUF-30. Compared with PEI-PUF-10, the adsorption rate was faster and the equilibrium time was shorter for PEI-PUF-30, which may be due to the high content of PEI and the easily accessible active sites. In order to insure to reach equilibrium at different experimental conditions, 80 min was set as equilibrium time for all other experiments.

Pseudo-first-order and pseudo-second-order kinetic models were investigated by fitting the experimental

data obtained from the batch method. The fitted plots of the pseudo-first-order and pseudo-second-order kinetics models are shown in Fig. 6. Table 2 shows the values of  $k_1$ ,  $k_2$  and  $q_e$  for the adsorption of Pb(II) on PEI-PUF-10 and PEI-PUF-30. It can be seen that both the pseudo-first-order and pseudo-second-order kinetics models fitted the data well with high regression values. However, the regression value of the pseudo-second-order model was a little higher than that of pseudo-first-order model. It indicated that the pseudo-second-order model can describe the adsorption kinetics of Pb(II) on PEI-PUF-10 and PEI-PUF-30 better.

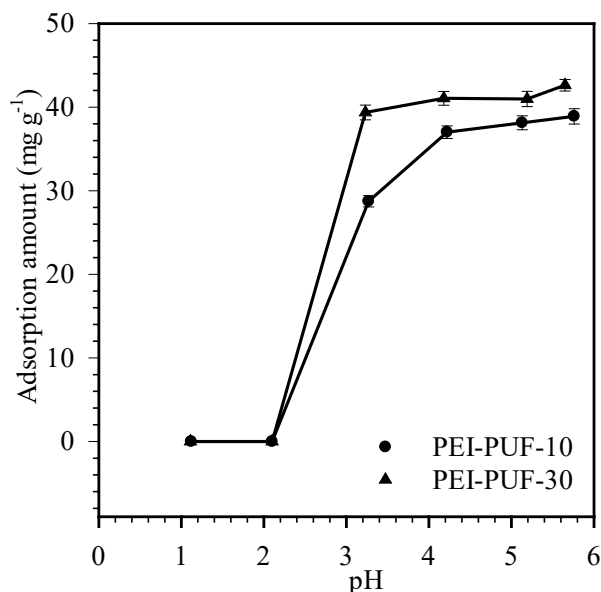


Fig. 4. Effect of pH on adsorption of Pb(II) by PEI-PUF-10 and PEI-PUF-30.

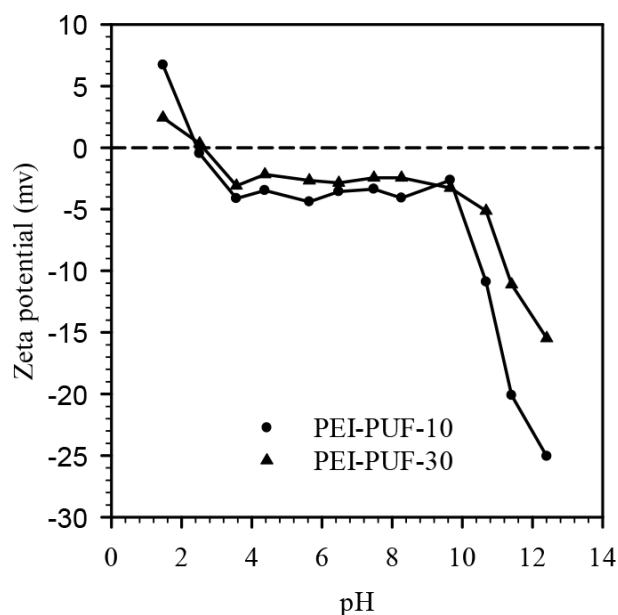


Fig. 5. Zeta potentials of PEI-PUF-10 and PEI-PUF-30 under different pH media.

### 3.4. Adsorption isotherms

Different initial concentration (20–350 mg·L<sup>-1</sup>) on the adsorption of Pb(II) by PEI-PUF-10 and PEI-PUF-30 were studied. The Langmuir adsorption isotherm model was applied to the adsorption data of the present work. Fig. 7 shows the Langmuir adsorption isotherms of Pb(II) on PEI-PUF-10 and PEI-PUF-30. The Langmuir model fitted the data well yielding high regression values, and the results are shown in Table 3. It indicated that the adsorption of Pb(II) on PEI-PUF-10 and PEI-PUF-30 was mainly homo-

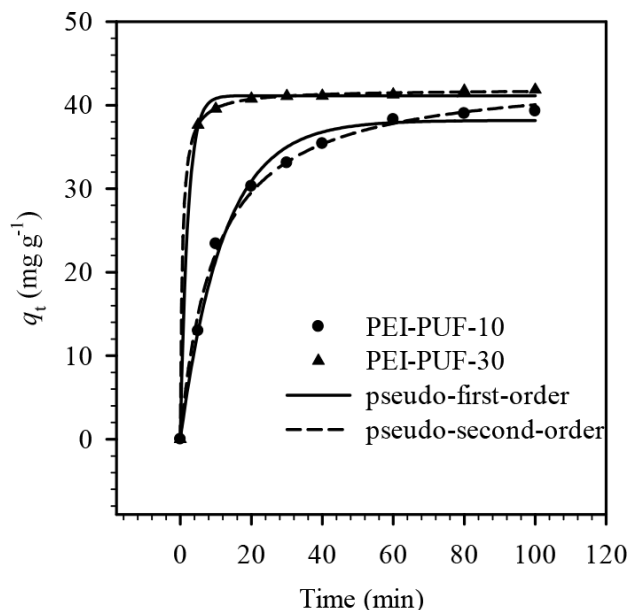


Fig. 6. Pseudo-first-order and pseudo-second-order kinetic model for adsorption of Pb(II) by PEI-PUF-10 and PEI-PUF-30.

geneous adsorption. The uptake of Pb(II) increased with increasing equilibrium concentration, and increased more rapidly for PEI-PUF-30 compared with PEI-PUF-10. It may be due to the high PEI content of PEI-PUF-30. The maximum adsorption capacities of Pb(II) on PEI-PUF-10 and PEI-PUF-30 were 98.1 and 183.0 mg g<sup>-1</sup>. It indicated that PEI-PUF-30 with high content of PEI is more suitable for Pb(II) removal from waste water. A comparison of the maximum adsorption capacity for Pb(II) on PEI-PUF-30 with those of other adsorbents reported by other researchers is shown in Table 4. It can be seen that the adsorbent used in this work is similar or even better in most cases compared with other adsorbents. Moreover, this adsorbent can make good use of waste PUF for waste reuse. PEI-PUF-30 is therefore a superior adsorbent for Pb(II) removal.

### 3.5. Adsorption thermodynamics

The effects of temperature on the adsorption of Pb(II) by PEI-PUF-10 and PEI-PUF-30 were investigated. The results showed that the adsorption amount of Pb(II) on PEI-PUF-10 and PEI-PUF-30 increased with the temperature increase, which indicated the uptake of Pb(II) was favorable at higher temperature. Thermodynamics analysis was performed to elucidate the inherent energetic changes associated with the adsorption of Pb(II) on PEI-PUF. The thermodynamic parameters such as Gibbs free energy change ( $\Delta G$ ), enthalpy change ( $\Delta H$ ) and entropy change ( $\Delta S$ ) were determined.  $\Delta G$ ,  $\Delta H$  and  $\Delta S$  can be calculated from the following equations:

$$\ln K_c = -\frac{\Delta H}{RT} + \frac{\Delta S}{R} \quad (4)$$

$$\Delta G = \Delta H - T\Delta S \quad (5)$$

where  $T$  is the absolute temperature (K),  $R$  is the gas constant (8.314 J mol<sup>-1</sup> K<sup>-1</sup>).  $K_c$  is the distribution coefficient which is

Table 2  
Pseudo-first-order and pseudo-second-order kinetic parameters for adsorption of Pb(II) on PEI-PUF-10 and PEI-PUF-30

Adsorbents	Pseudo-first-order			Pseudo-second-order		
	$q_e$ (mg g <sup>-1</sup> )	$k_1$ (h <sup>-1</sup> )	$R^2$	$q_e$ (mg g <sup>-1</sup> )	$k_2$ (g mg <sup>-1</sup> h <sup>-1/2</sup> )	$R^2$
PEI-PUF-10	38.17	0.083	0.9920	43.9	0.0023	0.9957
PEI-PUF-30	41.1	0.48	0.9982	41.9	0.042	0.9999

Table 3  
Langmuir adsorption isotherm constants for Pb(II) adsorption on PEI-PUF-10 and PEI-PUF-30

Adsorbents	$q_m$ (mg g <sup>-1</sup> )	$b$ (L mg <sup>-1</sup> )	$R^2$
PEI-PUF-10	98.1	0.16	0.990
PEI-PUF-30	183.0	0.04	0.997

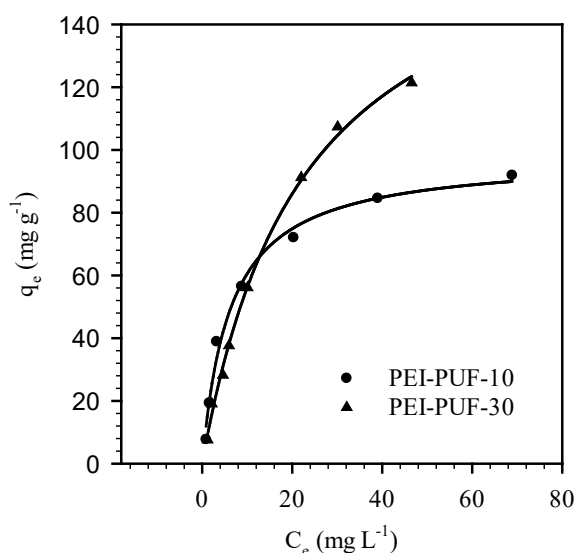


Fig. 7. Langmuir adsorption isotherms of Pb(II) on PEI-PUF-10 and PEI-PUF-30.

calculated as the ratio of Pb(II) equilibrium concentration in the adsorbents and aqueous phases.  $\Delta H$  and  $\Delta S$  can be obtained from the slope and intercept of the linear plot of  $\ln K_c$  versus  $1/T$ , as shown in Fig. 8.  $\Delta G$  can be calculated from Eq. (5). The determined thermodynamic parameters are shown in Table 5. The negative values of  $\Delta G$  indicated that the adsorption of Pb(II) on PEI-PUF was thermodynamically feasible and spontaneous. The derived  $\Delta G$  values became more negative with the increasing temperature, which indicated that the spontaneity and thermodynamic favorability of Pb(II) adsorption on PEI-PUF were enhanced with temperature. At the same temperature, the derived  $\Delta G$  values of PEI-PUF-30 became more negative than that of PEI-PUF-10, which indicated that the adsorption became more feasible for PEI-PUF-30 with high content of PEI. The positive values of  $\Delta H$  indicated that the adsorption process of Pb(II) on PEI-PUF progressed endothermically. Meanwhile, the positive values of  $\Delta S$  suggested that the adsorbed

Table 4  
Adsorption capacities of various adsorbents used for Pb(II) removal from aqueous solutions

Adsorbents	$q_{max}$ (mg g <sup>-1</sup> )	Reference
Polyvinyl alcohol/grapheme oxide-sodium alginate nanocomposite hydrogel	279.43	[40]
$\beta$ -cyclodextrin polymers	196.42	[41]
Amine functionalized porous organic polymer	523.6	[42]
Nitrogen-functionalized multiwalled carbon nanotubes	36.23	[15]
ZSM-5 zeolite	20.1	[16]
Functionalized NiFe <sub>2</sub> O <sub>4</sub> /MnO <sub>2</sub> nanocomposites	85.78	[7]
Bone ash/nanoscale zerovalent iron composite	160	[43]
Polyethylenimine-functionalized amorphous carbon	143	[44]
Polyethylenimine-bacterial cellulose bioadsorbent	141	[45]
PEI-PUF-30	183.0	This work

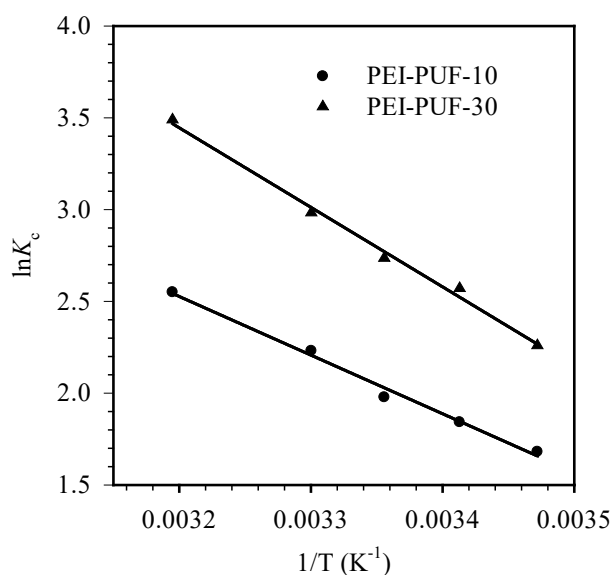


Fig. 8. Effect of temperature on the adsorption of Pb(II) by PEI-PUF-10 and PEI-PUF-30.

Table 5  
Thermodynamic parameters for Pb(II) adsorption by PEI-PUF-10 and PEI-PUF-30

Adsorbents	Temperature (K)	$\Delta G$ (kJ mol <sup>-1</sup> )	$\Delta H$ (kJ mol <sup>-1</sup> )	$\Delta S$ (J mol <sup>-1</sup> K <sup>-1</sup> )
PEI-PUF-10	288	-3.98	26.55	106.00
	293	-4.51		
	298	-5.04		
	303	-5.57		
	308	-6.10		
PEI-PUF-30	288	-5.43	36.02	143.92
	293	-6.15		
	298	-6.87		
	303	-7.59		
	308	-8.31		

Pb(II) presented a certain amount of freedom in the solid/solution interface, which confirmed the spontaneity of the endothermic Pb(II) adsorption process.

### 3.6. Regeneration and reusability

0.1 mol L<sup>-1</sup> EDTA was used as the desorption solutions. Five consecutive adsorption-desorption cycles were conducted to explore the reusability of PEI-PUF. The results are shown in Fig. 9. It was observed that after five cycles of adsorption-desorption with EDTA solution, the adsorption capacity of Pb(II) only lost 7.3% compared with the first adsorption, which indicated the good regeneration and reusability of PEI-PUF. Overall, PEI-PUF exhibits good reusability and can be repeatedly used for practical application.

## 4. Conclusions

PEI modified open-cell PUF adsorbents were successfully prepared and characterized by FTIR, FESEM, XPS and elementary analysis. PEI-PUF-10 and PEI-PUF-30 with different content of PEI were studied in the adsorption experiments. The prepared PEI-PUF-10 and PEI-PUF-30 had superior adsorption performance for Pb(II) compared with pristine PUF. The adsorption mechanism was mainly complexation followed by electrostatic interaction. The adsorption kinetics and isotherms data indicated that the Pb(II) adsorption followed pseudo-second-order kinetic and Langmuir isotherm models. The maximum adsorption capacities of Pb(II) on PEI-PUF-10 and PEI-PUF-30 were 98.1 and 183.0 mg g<sup>-1</sup>, respectively. PEI-PUF-30 with higher content of PEI exhibited a higher adsorption capacity than that of PEI-PUF-10. The adsorption of Pb(II) on PEI-PUF was highly pH dependent and endothermic. The pH<sub>zcp</sub> values of PEI-PUF were around 2.5, and the adsorption amount increased with the pH increase. The thermodynamic parameters of negative values of  $\Delta G$  and positive values of  $\Delta H$  suggested the spontaneous and endothermic nature of the adsorption process. After five cycles of adsorption/desorption, the adsorption capacity of Pb(II) on PEI-PUF-30

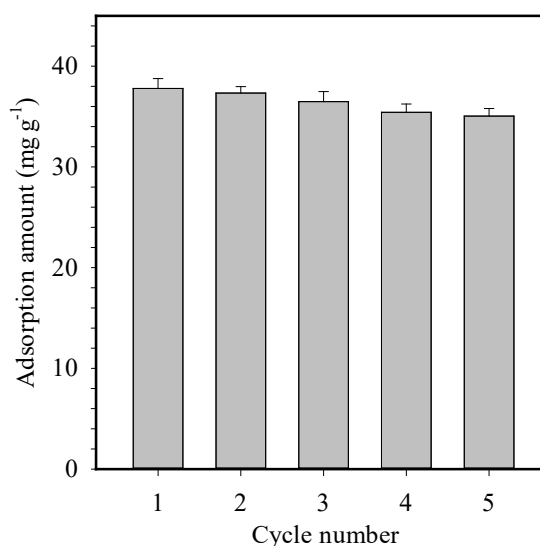


Fig. 9. The reusability of PEI-PUF-30 for the adsorption of Pb(II).

lost only 7.3% compared with the first adsorption. PEI-PUF exhibits good reusability.

## Acknowledgements

The work was supported by the National Natural Science Foundation of China (NOs. 21404053, 21501087), Promotive Research Fund for Excellent Young and Middle-Aged Scientists of Shandong Province (NO. BS2013CL035), Natural Science Foundation of Shandong Province (NO. ZR2017PB006), Natural Science Foundation of Ludong University (NOs. LY2013013, LY2013012).

## References

- [1] F. Mojoudi, A.H. Hamidian, N. Goodarziyan, S. Eagderi, Effective removal of heavy metals from aqueous solution by porous activated carbon/thiol functionalized graphene oxide composite, *Desal. Water Treat.*, 124 (2018) 106–116.
- [2] C. Sun, C. Li, R. Qu, Y. Zhang, B. Zhang, Y. Kuang, Syntheses of diethylenetriamine-bridged polysilsesquioxanes and their structure-adsorption properties for Hg(II) and Ag(I), *Chem. Eng. J.*, 240 (2014) 369–378.
- [3] J. Zhao, Y. Niu, B. Ren, H. Chen, S. Zhang, J. Jin, Y. Zhang, Synthesis of Schiff base functionalized superparamagnetic Fe<sub>3</sub>O<sub>4</sub> composites for effective removal of Pb(II) and Cd(II) from aqueous solution, *Chem. Eng. J.*, 347 (2018) 574–584.
- [4] C. Ji, S. Song, C. Wang, C. Sun, R. Qu, C. Wang, H. Chen, Preparation and adsorption properties of chelating resins containing 3-aminopyridine and hydrophilic spacer arm for Hg(II), *Chem. Eng. J.*, 165 (2010) 573–580.
- [5] A. Hosseini-Bandegharai, M. Karimzadeh, M. Sarwghadi, A. Heydarbeigi, S.H. Hosseini, M. Nedaie, H. Shoghi, Use of a selective extractant-impregnated resin for removal of Pb(II) ion from waters and wastewaters: Kinetics, equilibrium and thermodynamic study, *Chem. Eng. Res. Des.*, 92 (2014) 581–591.
- [6] Y. Liu, L. Xu, J. Liu, X. Liu, C. Chen, G. Li, Y. Meng, Graphene oxides cross-linked with hyperbranched polyethylenimines: Preparation, characterization and their potential as recyclable and highly efficient adsorption materials for lead(II) ions, *Chem. Eng. J.*, 285 (2016) 698–708.



- [7] B. Xiang, D. Ling, H. Lou, H. Gu, 3D hierarchical flower-like nickel ferrite/manganese dioxide toward lead (II) removal from aqueous water, *J. Hazard. Mater.*, 325 (2017) 178–188.
- [8] C.F. Carolin, P.S. Kumar, A. Saravanan, G.J. Joshiba, M. Nausshad, Efficient techniques for the removal of toxic heavy metals from aquatic environment: A review, *J. Environ. Chem. Eng.*, 5 (2017) 2782–2799.
- [9] M. Mesli, N.E. Belkhouche, Emulsion ionic liquid membrane for recovery process of lead. Comparative study of experimental and response surface design, *Chem. Eng. Res. Des.*, 129 (2018) 160–169.
- [10] Z. Zhang, L. Zhu, Y. Meng, S. Jia, Adsorption of methylene blue from aqueous solution by sol-gel silica doped with sec-octylphenoxyl acetic acid, *Desal. Water Treat.*, 108 (2018) 338–344.
- [11] Y. Niu, R. Qu, H. Chen, L. Mu, X. Liu, T. Wang, Y. Zhang, C. Sun, Synthesis of silica gel supported salicylaldehyde modified PAMAM dendrimers for the effective removal of Hg(II) from aqueous solution, *J. Hazard. Mater.*, 278 (2014) 267–278.
- [12] C. Zhang, M. Jin, C. Sun, R. Qu, Y. Zhang, Synthesis of polyamine-bridged polysiloxanes and their adsorption properties for heavy metal ions, *Environ. Prog. Sustain. Energy.*, 36 (2017) 1089–1099.
- [13] D. Lv, Y. Liu, J. Zhou, K. Yang, Z. Lou, S.A. Baig, X. Xu, Application of EDTA-functionalized bamboo activated carbon (BAC) for Pb(II) and Cu(II) removal from aqueous solutions, *Appl. Surf. Sci.*, 428 (2018) 648–658.
- [14] M.K. Uddin, A review on the adsorption of heavy metals by clay minerals, with special focus on the past decade, *Chem. Eng. J.*, 308 (2017) 438–462.
- [15] O.A. Oyetade, A.A. Skelton, V.O. Nyamori, S.B. Jonnalagadda, B.S. Martincigh, Experimental and DFT studies on the selective adsorption of Pb<sup>2+</sup> and Zn<sup>2+</sup> from aqueous solution by nitrogen-functionalized multiwalled carbon nanotubes, *Sep. Purif. Technol.*, 188 (2017) 174–187.
- [16] X. Wang, D. Shao, G. Hou, X. Wang, A. Alsaedi, B. Ahmad, Uptake of Pb(II) and U(VI) ions from aqueous solutions by the ZSM-5 zeolite, *J. Mol. Liq.*, 207 (2015) 338–342.
- [17] F.Q. An, Y. Wang, X.Y. Xue, T.P. Hu, J.F. Gao, B.J. Gao, Design and application of thiourea modified D301 resin for the effective removal of toxic heavy metal ions, *Chem. Eng. Res. Des.*, 130 (2018) 78–86.
- [18] Y. Niu, R. Qu, C. Sun, C. Wang, H. Chen, C. Ji, Y. Zhang, X. Shao, F. Bu, Adsorption of Pb(II) from aqueous solution by silica-gel supported hyperbranched polyamidoamine dendrimers, *J. Hazard. Mater.*, 244–245 (2013) 276–286.
- [19] J.O. Vinhal, C.F. Lima, R.J. Cassella, Polyurethane foam loaded with sodium dodecylsulfate for the extraction of 'quat' pesticides from aqueous medium: Optimization of loading conditions, *Ecotoxicol. Environ. Saf.* 131 (2016) 72–78.
- [20] C. Teodosiu, R. Wenkert, L. Tofan, C. Paduraru, Advances in preconcentration/removal of environmentally relevant heavy metal ions from water and wastewater by sorbents based on polyurethane foam, *Rev. Chem. Eng.*, 30 (2014) 403–420.
- [21] D. Yuan, T. Zhang, Q. Guo, F. Qiu, D. Yang, Z. Ou, A novel hierarchical hollow SiO<sub>2</sub>@MnO<sub>2</sub> cubes reinforced elastic polyurethane foam for the highly efficient removal of oil from water, *Chem. Eng. J.*, 327 (2017) 539–547.
- [22] K. Dong, F. Qiu, X. Guo, J. Xu, D. Yang, K. He, Polyurethane-attapulgite porous material: Preparation, characterization, and application for dye adsorption, *J. Appl. Polym. Sci.*, 129 (2013) 1697–1706.
- [23] J. Qin, F. Qiu, X. Rong, J. Yan, H. Zhao, D. Yang, Adsorption behavior of crystal violet from aqueous solutions with chitosan-graphite oxide modified polyurethane as an adsorbent, *J. Appl. Polym. Sci.*, 132 (2015) DOI: 10.1002/app.41828.
- [24] L. Kong, F. Qiu, Z. Zhao, X. Zhang, T. Zhang, J. Pan, D. Yang, Removal of brilliant green from aqueous solutions based on polyurethane foam adsorbent modified with coal, *J. Clean. Prod.*, 137 (2016) 51–59.
- [25] Z. Zhang, L. Zhu, J. Jin, Preparation of polyurethane foam adsorbents and their application on preconcentration/removal of metal ions, *Materials Review (A): Review Papers*. 31 (2017) 34–39 (in Chinese).
- [26] N. Burham, Separation and preconcentration system for lead and cadmium determination in natural samples using 2-aminoacetylthiophenol modified polyurethane foam, *Desalination*, 249 (2009) 1199–1205.
- [27] H. Sone, B. Fugetsu, S. Tanaka, Selective elimination of lead(II) ions by alginate/polyurethane composite foams, *J. Hazard. Mater.*, 162 (2009) 423–429.
- [28] S.H. Jang, B.G. Min, Y.G. Jeong, W.S. Lyoo, S.C. Lee, Removal of lead ions in aqueous solution by hydroxyapatite/polyurethane composite foams, *J. Hazard. Mater.*, 152 (2008) 1285–1292.
- [29] B. Liu, Y. Huang, Polyethyleneimine modified eggshell membrane as a novel biosorbent for adsorption and detoxification of Cr(VI) from water, *J. Mater. Chem.*, 21 (2011) 17413–17418.
- [30] S. Lagergren, Zur theorie der sogenannten adsorption gel ster stoffe, *Kungl. Svenska Vetensk. Handl.*, 24 (1898) 1–39.
- [31] Y.S. Ho, G. McKay, Pseudo-second order model for sorption processes, *Process Biochem.*, 34 (1999) 451–465.
- [32] S.M. Abdel Azeem, S.M. Mohamed Attaf, M.F. El-Shahat, Acetylacetone phenylhydrazone functionalized polyurethane foam: Determination of copper, zinc and manganese in environmental samples and pharmaceuticals using flame atomic absorption spectrometry, *React. Funct. Polym.*, 73 (2013) 182–191.
- [33] Y. Ma, W.J. Liu, N. Zhang, Y.S. Li, H. Jiang, G.P. Sheng, Polyethyleneimine modified biochar adsorbent for hexavalent chromium removal from the aqueous solution, *Bioresour. Technol.*, 169 (2014) 403–408.
- [34] X. Zhang, Z. Li, K. Liu, L. Jiang, Bioinspired multifunctional foam with self-cleaning and oil/water separation, *Adv. Funct. Mater.*, 23 (2013) 2881–2886.
- [35] J. Li, J.L. Gong, G.M. Zeng, P. Zhang, B. Song, W.C. Cao, H.Y. Liu, S.Y. Huan, Zirconium-based metal organic frameworks loaded on polyurethane foam membrane for simultaneous removal of dyes with different charges, *J. Colloid Interf. Sci.*, 527 (2018) 267–279.
- [36] Q. Zhu, Q. Pan, F. Liu, Facile removal and collection of oils from water surfaces through superhydrophobic and superoleophilic sponges, *J. Phys. Chem. C*, 115 (2011) 17464–17470.
- [37] H.C. Yang, J.L. Gong, G.M. Zeng, P. Zhang, J. Zhang, H.Y. Liu, S.Y. Huan, Polyurethane foam membranes filled with humic acid-chitosan crosslinked gels for selective and simultaneous removal of dyes, *J. Colloid Interf. Sci.*, 505 (2017) 67–78.
- [38] Q. Zhu, Y. Chu, Z. Wang, N. Chen, L. Lin, F. Liu, Q. Pan, Robust superhydrophobic polyurethane sponge as a highly reusable oil-absorption material, *J. Mater. Chem. A*, 1 (2013) 5386–5393.
- [39] M. Machida, T. Mochimaru, H. Tatsumoto, Lead(II) adsorption onto the graphene layer of carbonaceous materials in aqueous solution, *Carbon*, 44 (2006) 2681–2688.
- [40] Y. Yu, G. Zhang, L. Ye, Preparation and adsorption mechanism of polyvinyl alcohol/graphene oxide-sodium alginate nanocomposite hydrogel with high Pb(II) adsorption capacity, *J. Appl. Polym. Sci.*, 136 (2019) DOI: 10.1002/APP.47318.
- [41] J. He, Y. Li, C. Wang, K. Zhang, D. Lin, L. Kong, J. Liu, Rapid adsorption of Pb, Cu and Cd from aqueous solutions by  $\beta$ -cyclodextrin polymers, *Appl. Surf. Sci.*, 426 (2017) 29–39.
- [42] Y. He, Q. Liu, J. Hu, C. Zhao, C. Peng, Q. Yang, H. Wang, H. Liu, Efficient removal of Pb(II) by amine functionalized porous organic polymer through post-synthetic modification, *Sep. Purif. Technol.*, 180 (2017) 142–148.
- [43] A. Gil, M.J. Amiri, J. Abedi-Koupai, S. Eslamian, Adsorption/reduction of Hg(II) and Pb(II) from aqueous solutions by using bone ash/nZVI composite: effects of aging time, Fe loading quantity and co-existing ions, *Environ. Sci. Pollution Res.*, 25 (2017) 2814–2829.
- [44] M. El-Sayed, A.A. Nada, Polyethyleneimine-functionalized amorphous carbon fabricated from oil palm leaves as a novel adsorbent for Cr(VI) and Pb(II) from aqueous solution, *J. Water Process Eng.*, 16 (2017) 296–308.
- [45] X. Jin, Z. Xiang, Q. Liu, Y. Chen, F. Lu, Polyethyleneimine-bacterial cellulose bioadsorbent for effective removal of copper and lead ions from aqueous solution, *Bioresour. Technol.*, 244 (2017) 844–849.